On mass-conservation in high-order high-resolution rigorous remapping schemes on the sphere

Christoph Erath *

University of Colorado at Boulder and National Center for Atmospheric Research, Boulder, Colorado, USA

Peter H. Lauritzen

National Center for Atmospheric Research,[†] Boulder, Colorado, USA

Henry M. Tufo

University of Colorado at Boulder, Boulder, Colorado, USA

[*] *Corresponding author address:* Institute for Mathematics Applied to Geosciences (IMAGe) 1850 Table Mesa Drive, Boulder CO 80305, USA

E-mail: erath@ucar.edu

[†] The National Center for Atmospheric Research is sponsored by the National Science Foundation.

ABSTRACT

It is the purpose of this short article to analyze mass conservation in high-order rigorous remapping schemes, which contrary to flux-based methods, relies on elaborate integral constraints over overlap areas and reconstruction functions. For applications on the sphere these integral constraints may be violated primarily due to inexact or ill-conditioned integration and we propose a generic, local and multi-tracer efficient method that guarantees that the integral constraints are satisfied in discrete space irrespective of the accuracy of the numerical integration method and slight inaccuracies in the computation of overlap areas. We refer to this method as *enforcement of consistency* as it is based on integral constraints valid in continuous space. The consistency enforcement method is illustrated in idealized transport tests with CSLAM in HOMME (Conservative Semi-LAgrangian Multi tracer scheme in the High Order Method Modeling Environment) where the analytic integrals, that were found to be ill-conditioned at certain resolutions and flow conditions, have been replaced with robust quadrature. This violates mass-conservation, however, with the consistency enforcement method mass-conservation is inherent even with low-order quadrature and renders rigorous remap schemes such as CSLAM (that was previously limited to gnomonic cubed-sphere grids) mass-conservative on any spherical grid.

1. Introduction

The conservative transfer of quantities from one mesh to another has been extensively studied in Lagrangian hydrodynamic applications in Cartesian geometry since the pioneering work of Dukowicz (1984). Perhaps its first application to atmospheric transport in Cartesian geometry was by Rančić (1992). Rezoning or remapping on the sphere has also received considerable attention in the atmospheric sciences due to its applications in the conservative coupling of components in global climate system models (Jones 1999; Lauritzen and Nair 2008; Ullrich et al. 2009) and conservative semi-Lagrangian tracer transport on global domains (e.g., Lauritzen et al. 2010). Mass-conservation in rigorous remapping schemes is more stringent compared to flux-based discretizations (e.g., Lauritzen et al. 2011b). In flux-form discretizations any flux, as long as the flux through a cell edge is the same with opposite sign for the neighboring cell sharing that edge, will lead to mass-conservation. Mass-conservation in high-order remap schemes relies on satisfying integral constraints for the reconstruction function over overlap areas that trivially hold in continuous space; however, in the high-order high-resolution parallel implementation of CSLAM (Conservative Semi-LAgrangian Multi tracer scheme, Lauritzen et al. 2010) on the cubed-sphere (Erath et al. 2012) it was found that these constraints are not necessarily satisfied in discretized space mainly due to ill-conditioning of analytic line-integrals on the sphere (involving differencing trigonometric functions of similar magnitude). Simply switching integration to more robust quadrature methods may lead to violation of mass-conservation. This has motivated a rigorous analysis of mass-conservation in remap schemes and the derivation of a generic consistency-enforcement method that ensures mass-conservation regardless of numerical method chosen for the identification and integration of overlap areas. This allows for implementing remapping schemes which are much more robust against several approximation errors that may appear in the implementations of high-resolution high-order remapping algorithms on the sphere.

The content of this paper is organized as follows. Section 2 describes the remapping problem and provides a mass-conservation analysis. In Section 3 we apply the theoretical results and introduce the mass consistency enforcement. Numerical examples confirm the robustness of our approach. Conclusions can be found in Section 4.

2. The remapping problem and mass-conservation

The discussion below focusses on the remap discretization of the transport equation, however, the derivations generalize to the more general remapping problem between two grids.

a. High-order remapping

The upstream remap or cell-integrated Lagrangian discretization of the transport equation for a passive and inert scalar ψ in cell k can be written as

$$\overline{\psi}_k^{n+1} \, |A_k| = \left\{ \sum_{\ell \in \mathcal{L}_k} \left[\sum_{p+q \leq h} c_\ell^{(p,q)} \, \omega_{k\ell}^{(p,q)} \right] \right\}, \tag{1}$$

(equation 15 or 38 in Lauritzen et al. 2010), where $\overline{\psi}_k^{n+1}$ is the cell-averaged value of ψ at time-level $(n+1)$ over cell A_k with corresponding area $|A_k|$. The definition of $c_\ell^{(p,q)}$ and $\omega_{k\ell}^{(p,q)}$ requires the introduction of more notation.

The upstream Lagrangian area that arrives at Eulerian cell A_k after one time-step Δt is denoted a_k, see Figure 1(a). The overlap area between upstream cell a_k and Eulerian cell A_ℓ is denoted $a_{k\ell}$ and mathematically defined as

$$a_{k\ell} = a_k \cap A_\ell .$$

The set of indices for Eulerian cells that a_k overlaps is denoted

$$\mathcal{L}_k = \{\ell | a_{k\ell} \neq \emptyset\} .$$

A high-order finite-volume scheme based on rigorous remapping involves a high-order reconstruction function in each Eulerian cell A_k (for a review see, e.g., Lauritzen et al.

2011b). For simplicity, assume that a polynomial reconstruction on the form

$$\psi_k(x,y) = \sum_{p+q\leq h} c_k^{(p,q)} x^p y^q,$$

is used, where h is the degree of the polynomial with $p, q, h \in \mathbb{N}_0$ and $c_k^{(p,q)}$ are the reconstruction coefficients. In Lagrangian remap schemes the constant coefficient $c_k^{(0,0)}$ is chosen such that $\psi_k(x,y)$ integrated over the Eulerian cell A_k yields the cell-averaged mass $\overline{\psi}_k|A_k|$ (as is the case in continuous space):

$$\sum_{p+q\leq h} c_k^{(p,q)} m_k^{(p,q)} |A_k| = \overline{\psi}_k^n |A_k|, \tag{2}$$

where $m_k^{(p,q)}$ is the discretization of the integral

$$\frac{1}{|A_k|}\int_{A_k} x^p y^q \, dA \tag{3}$$

over Eulerian cell A_k. For fully two-dimensional polynomial reconstructions of degree 2 ($h = 2$) choices of $c^{(0,0)}$ are given in Ullrich et al. (2009, 2012).

The discretization of the integral

$$\int_{a_{k\ell}} x^p y^q \, dA,$$

over overlap area $a_{k\ell}$ is denoted $\omega_{k\ell}^{(p,q)}$. This concludes the description of the terms involved in the forecast equation (1).

b. Conservation of mass in rigorous remapping schemes

Mass is conserved globally if total mass at time level $n+1$ and n are equal, which simply reads

$$\sum_k \overline{\psi}_k^{n+1} |A_k| = \sum_k \overline{\psi}_k^n |A_k|. \tag{4}$$

In the following we demonstrate what conditions in discretization spaces must be fulfilled for mass to be conserved in rigorous remap schemes. First the forecast equation for $\overline{\psi}_k^{n+1}$

given in (1) is substituted on the left-hand side of (4)

$$\sum_k \overline{\psi}_k^{n+1} |A_k| = \sum_k \left\{ \sum_{\ell \in \mathcal{L}_k} \left[\sum_{p+q \leq h} c_\ell^{(p,q)} \, \omega_{k\ell}^{(p,q)} \right] \right\}. \tag{5}$$

The right-hand side of (5) may be written as

$$\begin{aligned} \sum_k \overline{\psi}_k^{n+1} |A_k| &= \sum_k \left\{ \sum_{\ell \in \mathcal{E}_k} \left[\sum_{p+q \leq h} c_k^{(p,q)} \, \omega_{\ell k}^{(p,q)} \right] \right\} \\ &= \sum_{p+q \leq h} \left[\sum_k c_k^{(p,q)} \sum_{\ell \in \mathcal{E}_k} \omega_{\ell k}^{(p,q)} \right]. \end{aligned} \tag{6}$$

Note that the subscript $k\ell$ have been swapped to ℓk: instead of summing over Eulerian indices that the upstream cell spans we sum over overlap areas that have non-empty overlap with Eulerian cell k, see also Figure 2(b),

$$\mathcal{E}_k = \left\{ \ell | a_{\ell k} \cap A_k \neq \emptyset \right\}. \tag{7}$$

Note that in the above notation: If

$$\sum_{\ell \in \mathcal{E}_k} \omega_{\ell k}^{(p,q)} = m_k^{(p,q)} |A_k| \qquad \text{for } p+q \leq h. \tag{8}$$

then the right-hand side of (6) becomes

$$\sum_k \overline{\psi}_k^{n+1} |A_k| = \sum_{p+q \leq h} \left[\sum_k c_k^{(p,q)} m_k^{(p,q)} |A_k| \right], \tag{9}$$

and if $c_k^{(0,0)}$ satisfies the 'mass-conservation constraint' in (2), we recover (4) by substituting (2) on the right-hand side of (9).

In other words, the discretized scheme must satisfy (8) for mass to be conserved globally and locally. For $p = q = 0$ that is

$$\sum_{\ell \in \mathcal{E}_k} |a_{\ell k}| = |A_k|,$$

which simply states that the overlap areas $a_{\ell k}$ that span the Eulerian cell A_k sum up to the area of the Eulerian cell k (a graphical illustration is given in Figure 2). Similar arguments hold for the higher-order moments ($p + q > 0$).

3. Numerical implementation issues

For numerical implementations of remapping schemes the constraint (8) is crucial for inherent mass-conservation. There can be several sources of error for the violation of (8). The most obvious source of error is the numerical approximation of the moment integral over the Eulerian area (3) which may not exactly equal the same quantity (in continuous space) computed in terms of a sum over overlap areas that collectively span the same Eulerian area (Figure 2). In other words, the same quantity is inherently computed in two different ways in the remap algorithm and they may differ due to:

- Inexact integration (in particular on the sphere where polynomial reconstruction functions lead to integration of non-polynomials due to metric terms), such as quadrature or ill-conditioned analytic expressions for the integrals. While high-order quadrature will accurately approximate the weights, the errors may still be above machine precession and lead to a slow accumulation of errors that may result in above machine round-off violation of mass-conservation in long simulations.

- Inaccuracies in the search algorithm that identifies overlap areas (crossings between a Lagrangian cell side and a coordinate line may be computed twice by neighboring Lagrangian cells and may differ slightly).

- Parallel implementation errors where it is common practice to compute the same quantities (in continuous space) on different cores to reduce the number of communications to a minimum. In case of a cubed-sphere grid they might be computed on different projections, such as departure location for points shared by two cubed-sphere edges.

While we acknowledge that the two latter items may be eliminated by very careful implementations, it is likely going to impact parallel efficiency and lead to increased algorithm complexity. In any case we may completely eliminate this source of error by enforcing consistency locally, that is, by scaling of $\omega_{\ell k}^{(p,q)}$:

$$\widetilde{\omega}_{\ell k}^{(p,q)} = \omega_{\ell k}^{(p,q)} \frac{m_k^{(p,q)}}{\sum_{i \in \mathcal{E}_k} \omega_{ik}^{(p,q)}}, \tag{10}$$

so that (8) is fulfilled. In words, it is ensured in discretized space that the integrals of any moment over overlap areas (belonging to different upstream Lagrangian cells) that span Eulerian cell k sum to the integral of the same moment over the same Eulerian cell k but computed as one integral[1]. We refer to this method as consistency enforcement rather than a 'fixer' as it is based on fulfilling integral properties that hold in continuous space and thus spring from physical constraints and not from 'ad hoc' mass-restoration ideas. We stress that this enforcement is local and therefore also suitable for parallel codes without having an extra expensive communication. Also, the scaling of the weights must only be performed once for all fields that are being remapped and it is therefore multi-tracer efficient.

a. *An example*

We illustrate the consistency problem and consistency enforcement method with CSLAM. The weights over $a_{k\ell}$ are computed in terms of line integrals in CSLAM. To ensure mass conservation line integrals overlapping Eulerian lines, see Figure 1(b), were computed analytically in the original formulation of CSLAM so that the sum of the line-segments that span an Eulerian cell exactly integrate the reconstruction function to the cell-average value[2] (2). Unfortunately, these analytical expressions can become ill-conditioned in particular the higher-order moments at high resolution (see equation (32) and (33) in Lauritzen et al. 2010). A similar analytical expression can be found in Erath et al. (2009) which becomes numerical unstable for high resolution meshes. As proposed in Erath et al. (2009) one can replace the analytical integral by quadrature to get a robust approximation. As discussed above, in

[1] in HOMME-CSLAM the weights for the latter integral are pre-computed as they, contrary to the overlap areas, are not flow-dependent.

[2] Note that line-integrals not overlapping grid lines cancel between neighboring Lagrangian cell sides since the line-integrals are computed in both directions (and are hence equal with opposite sign) and added

spherical geometry, this can lead to mass-conservation errors unless the general consistency enforcement (10) method is used. We illustrate this in the next section.

b. Numerical experiments

For the following tests we use the third-order accurate CSLAM implementation in HOMME (High Order Method Modeling Environment, Dennis et al. 2005, 2012) which is documented in Erath et al. (2012). HOMME is a dynamical core in NCAR's Community Atmosphere Model (CAM). The tests are performed on the sphere with an analytical wind field and Gaussian surfaces as initial fields (wind field case 3 in Nair and Lauritzen 2010). We chose a time-step of 800 seconds at resolution 1.12° resulting in a maximum Courant number of 0.8. The Gaussian surfaces are infinitely smooth and leads to the optimal convergence rate of 3 with CSLAM when no shape-preserving filter is applied (Figure 4 in Lauritzen et al. 2012). All tests are run on an equi-distant gnomonic grid and air-mass and tracer mass are coupled as described in Appendix B of Nair and Lauritzen (2010). We stress that our consistency enforcement does not affect the coupling since the weights are re-used for both, the air-mass and tracer mass. No differences (up to machine precision) can be observed. Consequently a constant mixing ratio is also preserved with consistency enforcement. A constant air-mass, however, is not completely preserved for both variants, the version with analytical line integrals and the version with consistency enforcement; e.g., the changes for the scheme with our consistency enforcement and two Gaussian points compared to the version with analytical line integrals are of order 10^{-6}, which decreases with resolution.

Since the analytic evaluation of the line-integrals is ill-conditioned, which is manifested through simulation instability under certain flow conditions and resolutions, we replace the analytic integrals used in the original CSLAM with two or four point Gaussian quadrature and run the model with and without consistency enforcement. Figure 3 shows the relative mass error as a function of time step index. As expected mass errors with two quadrature points are significant: $\mathcal{O}(10^{-6})$ after twelve days of simulation (Figure 3(a)). Increasing the number of quadrature points to four (thereby increasing computational cost) reduces the relative mass-errors significantly to $\mathcal{O}(10^{-11})$ (Figure 3(b)); but still above machine round-off and the error could potentially accumulate over a typical climate scale simulation on the order of 10 years and more. When using the consistency enforcement algorithm the relative mass errors are around machine round-off: $\mathcal{O}(10^{-13})$ at day 12 of the simulation.

To investigate if the consistency enforcement algorithm affects accuracy we compute L^1, L^2, and L^∞ error norms at day 12 at resolutions ranging from 2.25° to 0.07° keeping the Courant number with 0.8 fixed (Figure 4). The rates of convergence remain third-order without a shape-preserving filter, and (almost) third-order (L^1), second-order (L^2) and 3/2-order (L^∞) with a shape-preserving filter as for the original (and less robust) CSLAM implementation using analytic line-integrals. Shape-preservation and the absolute L^1, L^2, and L^∞ errors (up to machine precision) are unaffected by the consistency enforcement algorithm (not shown).

Note that in the original formulation of CSLAM mass-conservation relied on the analytical integration along line-segments coinciding with grid lines which was possible on the gnomonic cubed-sphere grid (Ullrich et al. 2009). This limited the application of CSLAM to a special class of grids. With the consistency enforcement algorithm integration over over-lap areas can be replaced with quadrature and thereby allows for CSLAM to be implemented on any spherical grid and still be inherently mass-conserving. Higher-order edge approximations introduced in the context of simplified flux-form CSLAM (Ullrich et al. 2012) may also be applied in Lagrangian CSLAM using the consistency enforcement method for mass-conservation.

4. Conclusions

Based on a rigorous analysis of mass-conservation in remapping schemes we have derived a mandatory condition to achieve mass-conservation based on integral constraints valid in continuous space. Our proposed consistency enforcement is generic and applicable in any remapping algorithm. The integration over overlap areas can be performed with inexact quadrature while still retaining inherent mass-conservation. The consistency enforcement is completely local making it also attractive for parallel codes, and shape-preserving filters are not affected by the consistency enforcement algorithm. Idealized transport tests using CSLAM in HOMME illustrate how conservation of mass is violated when replacing analytical line-integrals (that are ill-conditioned under certain flow conditions and resolutions) with quadrature and that the consistency enforcement algorithm restores inherent mass-conservation without degrading simulation accuracy.

Acknowledgments.

The first author is funded by DOE BER Program DE-SC0006959. The authors thank Ramachandran D. Nair (National Center for Atmospheric Research) and Mark A. Taylor (Sandia National Laboratories) for many fruitful discussions. The authors gratefully acknowledge the three anonymous reviewers for their helpful comments.

REFERENCES

Dennis, J. M., A. Fournier, W. F. Spotz, A. St-Cyr, M. A. Taylor, S. J. Thomas, J. Stephen, and H. Tufo, 2005: High-Resolution Mesh Convergence Properties and Parallel Efficiency of a Spectral Element Atmospheric Dynamical Core. *Int. J. High Perform. Comput. Appl.*, **19**(3): 225-235.

Dennis, J. M., J. Edwards, K. J. Evans, O. Guba, P. H. Lauritzen, A. A. Mirin, A. St-Cyr, M. A. Taylor, and P. H. Worley, 2012: CAM-SE: A scalable spectral element dynamical core for the Community Atmosphere Model. *Int. J. High Perform. Comput. Appl.*, **26**(1): 74-89.

Dukowicz, J. K., 1986: Conservative rezoning (remapping) for general quadrilateral meshes. *J. Comput. Phys.*, **54**(3): 411-424.

Erath, C., S. Ferraz-Leite, S. A. Funken, and D. Praetorius, 2009: Energy norm based a posteriori error estimation for boundary element methods in two dimensions. *Appl. Numer. Math.*, **59**(11):2713–2734.

Erath, C., P. H. Lauritzen, J. H. Garcia, and H. M. Tufo, 2012: Integrating a scalable and efficient semi-Lagrangian multi-tracer transport scheme in HOMME. *Procedia Computer Science*, **9**, 994–1003.

Jones, P. W., 1999: First- and second-order conservative remapping schemes for grids in spherical coordinates. *Mon. Wea. Rev.*, **127**, 2204–2210.

Lauritzen, P. H. and R. D. Nair, 2008: Monotone and conservative Cascade Remapping between Spherical grids (CaRS): Regular latitude-longitude and cubed-sphere grids. *Mon. Wea. Rev.*, **136**, 1416–1432.

Lauritzen, P. H., R. D. Nair, and P. A. Ullrich, 2010: A conservative semi-Lagrangian multi-tracer transport scheme (CSLAM) on the cubed-sphere grid. *J. Comput. Phys.*, **229**, 1401–1424.

Lauritzen, P. H., W. C. Skamarock, M. J. Prather, and M. A. Taylor, 2012: A standard test case suite for two-dimensional linear transport on the sphere. *Geosci. Model Dev.*, **5**, 887-901.

Lauritzen, P. H., P. A. Ullrich, and R. D. Nair, 2011b: Atmospheric transport schemes: desirable properties and a semi-Lagrangian view on finite-volume discretizations, in: P.H. Lauritzen, R.D. Nair, C. Jablonowski, M. Taylor (Eds.), Numerical techniques for global atmospheric models. *Lecture Notes in Computational Science and Engineering, Springer, 2011*, **80**.

Nair, R. D., and P. H. Lauritzen, 2010: A class of deformational flow test cases for linear transport problems on the sphere. *J. Comput. Phys.*, **229**, 8868–8887.

Rančić, M., 1992: Semi-Lagrangian piecewise biparabolic scheme for two-dimensional horizontal advection of a passive scalar. *Mon. Wea. Rev.*, **120**, 1394-1405.

Ullrich, P. A., P. Lauritzen, and C. Jablonowski, 2012: Some considerations for high-order ‘incremental remap’-based transport schemes: edges, reconstructions and area integration. *Int. J. Numer. Meth. Fluids*.

Ullrich, P. A., P. H. Lauritzen, and C. Jablonowski, 2009: Geometrically exact conservative remapping (GECoRe): Regular latitude-longitude and cubed-sphere grids. *Mon. Wea. Rev.*, **137**(6), 1721–1741.

List of Figures

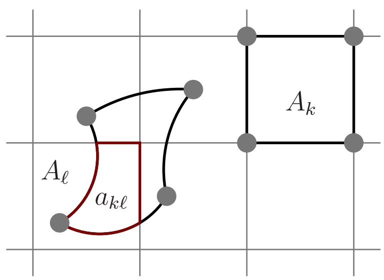

(a) Numerical integral over $a_{k\ell}$.

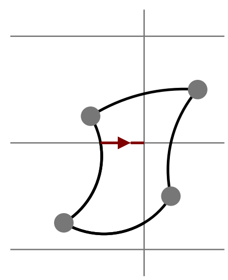

(b) Analytical line integral approach for this segment.

FIG. 1. (a) A graphical illustration of CSLAM that tracks Eulerian cell A_k upstream a_k. Since reconstruction functions are discontinuous at Eulerian cell boundaries the upstream integral over a_k is split into overlap integrals between a_k and Eulerian cell A_ℓ: $a_{k\ell}$. (b) Area integration is performed via line-integrals in CSLAM. In the original formulation of CSLAM line-integrals overlapping Eulerian grid lines where computed analytically on the sphere to ensure global mass-conservation.

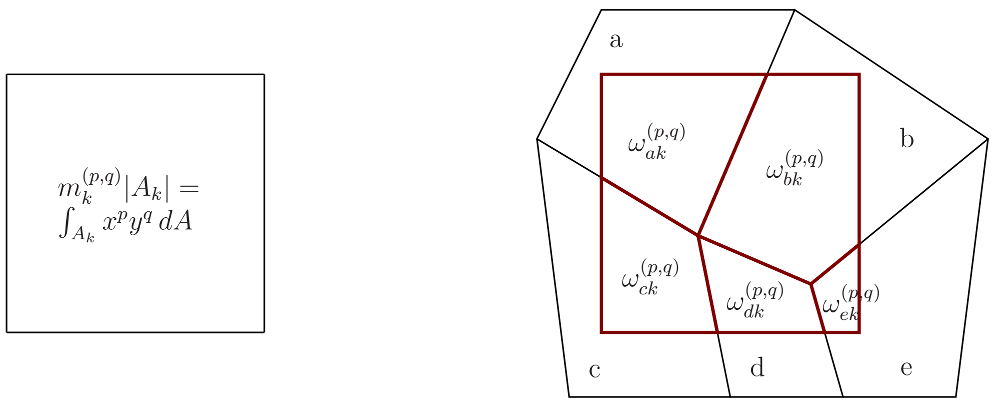

(a) Eulerian cell A_k.

(b) Overlap $\mathcal{E}_k$ of A_k.

FIG. 2. The condition (8), on which the consistency enforcement method is based, states that the integral of a moment over the Eulerian cell (a) must equal the sum of integrals of that moment over overlap areas that span the Eulerian cell ($A_k = a_{ak} \cup a_{bk} \cup a_{ck} \cup a_{dk} \cup a_{ek}$) in (b) to ensure mass conservation. Note that the different overlap areas belong to different upstream cells.

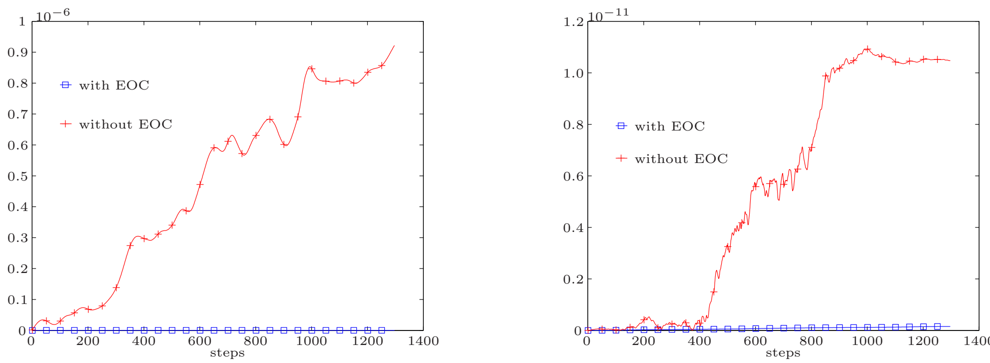

(a) Two Gaussian points for line integrals.

(b) Four Gaussian points for line integrals.

Fig. 3. The relative mass error for CSLAM in HOMME using line integral approximation with two and four Gaussian points for a 1.12° mesh with and without enforcement of consistency (EOC).

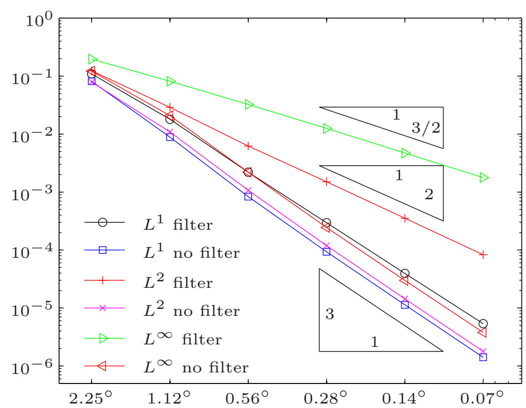

FIG. 4. The plot shows the convergence order of different error norms for our test example using line integral approximation with two Gaussian points and manipulation the weights, consistency enforcement (10). In particular, the rates of convergence remain third-order without a shape-preserving filter, and (almost) third-order (L^1), second-order (L^2) and 3/2-order (L^∞) with a shape-preserving filter as for the original (and less robust) CSLAM implementation using analytic line-integrals (not shown).